Predetection Recording and Dropouts

A. Slekys
Communications Systems Research Section

Predetection recording of spacecraft telemetry data allows for possible future analysis of data records in the event of failures of transmitted signals. Dropouts occurring in the playback process necessarily cause loss of information and, more importantly, loss of time synchronization with the remaining data. The object of this study is to show that, with proper digital handling of a timing signal initially recorded along with telemetry data using a device incorporating a proposed digital dropout detector, time synchronization can be maintained throughout dropouts of lengths less than 100 ms, within some small probability of error. Uses extend to recording of planetary entry low-rate and very long baseline interferometry data and, in particular, to planetary radio occultation information, which is already recorded with a timing signal on the same tape track.

I. Introduction

Currently, the DSN operates with more than one ground station tracking during critical phases of a spacecraft mission. This technique ensures that an entire ground station is available as backup if any failure occurs at the prime tracking station. The ground-based equipment, however, is designed to process the normal signal with small ability to accommodate changes in the spacecraft signals. Hence, it is rendered useless if failures of signal data rates or subcarriers, for example, occur during tracking. Recovery of the data transmitted during such a failure can be achieved if the spacecraft signal is continuously recorded on analog magnetic tape at intermediate frequency, before any subcarrier or data demodulation stages. Linear direct magnetic recording utilizing wideband instrumentation recorders such as the Ampex FR 1400 units presently installed at DSN stations is a cost-effective way of creating real-time predetection telemetry data records for future analysis. Imperfect tape drives and the imperfect magnetic recording medium cause tape speed variations, or flutter, and random data dropouts (Ref. 1), respectively. Loss of some data and, more importantly after a dropout, loss of synchronization with the subcarrier, bit, word, and frame syncs are the detrimental results.

A realistic solution to this problem is to record a sinusoidal reference signal on the same tape track with the data. Due to the present limitations on speed of data reconstruction equipment, there needs to be a speed reduction from 304.8 cm/s (120 ips) at record to 4.76 cm/s

(1⅞ ips) at playback. Flutter frequency modulates the reproduced signal at the low playback rate, necessitating some type of flutter frequency model if the timing sequence is to be predictable during and after a dropout.

This article assumes that the effective flutter can be approximated as a single-frequency FM modulating signal. Results of frequency and time-domain analyses of a reproduced sinusoid are shown, verifying the assumption for short time intervals (<100 ms). Computer simulation of a digital dropout detector, consisting essentially of a phase discriminator and a function generator, the latter incorporating the appropriate flutter model, is described. Probability density curves of the phase errors occurring during randomly initiated dropouts, of duration less than 100 ms, are presented. Applications extend to recording of planetary entry low-rate data, two station and very long baseline interferometry (VLBI) data, and also to planetary radio occultation experiment IF. The latter is presently detected and then recorded along with a timing signal on the same tape track. Occultation information lies primarily in the phase variations of the signal, making information extraction very vulnerable to both flutter and dropouts.

II. Frequency and Time Domain Analysis of Flutter

A. Frequency Analysis

Most approaches (Refs. 2 and 3) characterize flutter as a random Gaussian process, with a rather uniformly distributed power spectrum, from 1 Hz to 10 kHz. In this analysis, the intention is to establish that flutter can be approximated as a single-frequency FM modulating signal.

A timing sinusoid with a frequency of 320 kHz was recorded at 304.8 cm/s (120 ips) and played back at 4.76 cm/s (1⅞ ips), resulting in a flutter-modulated signal centered at 5 kHz. This was then sampled at 20 kHz, and the data were used in a computer routine in order to isolate the flutter sidebands.

A Fast Fourier Transform (FFT) computer algorithm was then applied to the sampled data; Fig. 1, representing 15 averaged spectra, clearly shows the predominant playback flutter sidebands, displaced 7.5 Hz from the center frequency, in this case 4994.83 Hz. The resolution of this particular FFT was set to 0.57 Hz, with 2048 points used. The most immediate side lobes around each of the major peaks are displaced by about 0.9 Hz and believed to be due to the record flutter, affecting the playback flutter as well as the carrier. The record flutter is substantially smaller than the playback flutter, supporting the view that at high speeds the tape drive is more linear.

B. Time Domain Analysis

A series of second-order Chebyshev polynomials were fitted to the original sampled timing sinusoid for every cycle of the sinusoid. Curves were fitted to each set of 4 sample points for every successive point, thereby resulting in a set of values of crossover times at each half-cycle of the function. These values were correlated for similarity and then averaged to give the net phase response of the sinusoid, with an estimated error of ± 10 degrees for every 180-degree phase interval. Figure 2 is a block diagram of the program.

The ideal phase $\omega_0' t$ (where $\omega_0' = 4995$ Hz from the FFT analysis) was subtracted from the net phase estimate $\hat{\phi}(t)$ to give $\hat{\theta}(t)$, an estimate of the phase variations due to flutter. A continuous average of $\hat{\theta}(t)$ with an averaging period of 50 cycles of the original sinusoid (about 0.01 s) resulted in the phase function $\hat{\theta}_A(t)$. As expected, it was found that $\hat{\theta}_A(t)$ is the sum of several sinusoids. The predominant term is of the form $K_m(t) \sin(\omega_m t + \alpha_m)$, where ω_m, agreeing with the FFT, is 7.5 Hz, and $K_m(t)$ varies between about 1.0 and 2.0 radians.

Three other sinusoidal components were detected: one continuous term at a frequency of 0.2 Hz and amplitude of about 1.7 radians, and two lesser sinusoids, one at 0.5 Hz ($\sim$0.3 radians), and the other at 1.73 Hz ($\sim$0.8 radians), which alternated with a period of 0.5 s. It was difficult to accurately define these latter amplitudes due to the predominance of the 7.5-Hz term with its large varying amplitude. These lower frequency terms did not show up in the FFT analysis, due to the resolution limitations in defining the spectrum.

III. Discussion of Results

The main playback flutter component at 7.5 Hz was traced to the drive motor, which, at a tape speed of 4.76 cm/s (1⅞ ips), rotates at 7.5 rps (450 rpm) in an Ampex FR 1400 machine, the type on which the signal was originally reproduced. At the record speed of 304.8 cm/s (120 ips), the tape drive motor rotates at 3600 rpm. This translates down to a frequency of about 0.9 Hz at a playback speed of 4.76 cm/s (1⅞ ips), agreeing with the spectrum record flutter value.

The continuous 0.2-Hz component may be due to the irregular rotation of the 25.4-cm (10-in.) takeup reel on

playback, which rotates at about 0.12 rps when empty and at 0.06 rps when full. This requires that the reel have two "bumps" occur for every revolution.

If the phase were observed for a longer period of time (i.e., the length of the tape), the frequency of this component should decrease to about 0.1 Hz. The other two alternating low-frequency signals, each present for about 0.5 s, were not traced to any specific mechanical rotation. In any event, the speed control built into the machine cannot compensate for these low-frequency flutter components.

IV. Dropout Detector Simulation

Several tracking devices were simulated on a computer, utilizing the same sampled sinusoid data. They all basically performed the function of extracting the average phase and frequency variations $\hat{\theta}_A(t)$ and $\hat{\theta}_A(t)$ as shown in Fig. 2. Whenever a dropout occurred, a sine function was then generated, in the form $\hat{\theta}_e(t) = K_m(t) \sin(\omega_m t + \alpha_m)$. For any dropout, $K_m(t)$ was set equal to the average of the magnitudes of all the preceding maxima and minima values of $\hat{\theta}_A(t)$. The distribution of these magnitudes was observed to be unevenly spread about 1.5 radians, with a maximum deviation of ± 0.5 radians. ω_m was in turn set equal to the rate of change of the most recent pair of maximum and minimum values of $\hat{\theta}_A(t)$. The resulting model phase values $\hat{\theta}_e(t)$ were compared at crossover times of the real phase function $\hat{\theta}(t)$, and the errors for each half-cycle of the sinusoid obtained. Figure 3 shows the measured probability density of phase error for two typical dropouts. The dropout intervals were both 100 ms, resulting in sample sets of about 1000 half-cycles, with error windows of 5 degrees used in establishing phase error magnitudes. It should be noted that for the Rayleigh-type density curve, the majority of error values is concentrated in the region of less than 20 degrees, while the other curve exhibits a broader error distribution, with a secondary peak in the range of 35 to 40 degrees. It was found that this latter curve represents a time interval during which there is a rapid rate of change in the magnitudes of the maximum and minimum values of $\hat{\theta}_A(t)$, resulting in a higher probability of error for the estimated value of $K_m(t)$ used in the model, and hence a larger error distribution. During both dropouts, the magnitudes of the phase errors tended to increase with the length of time of dropout, with errors exceeding 20 degrees occurring typically well after 50 ms.

Hence, this simple form of detector, containing essentially a phase discriminator and a sine function generator, could track through a dropout of length 100 ms or less, predicting the number of lost timing pulses (180 degrees apart) with a maximum error of ± 60 degrees for any one pulse.

References

1. Van Keuran, W., "An Examination of Dropouts Occurring in the Magnetic Recording and Reproduction Process," JPL preprint No. 656 (H-5), *Audio Eng. Soc.*, April 28–May 1, 1969.
2. Abramson, N., "Bandwidth and Spectrum of Phase and Frequency Modulated Waves," *IEEE Trans. Comm. Sys.*, Vol. CS-II, pp. 407–414, Dec. 1963.
3. Ratz, A. G., "The Effect of Tape Transport Flutter on Spectrum and Correlation Analysis," *IEEE Trans. Sp. Elec. Tel.*, Vol. SET-10, pp. 129–134, Dec. 1964.

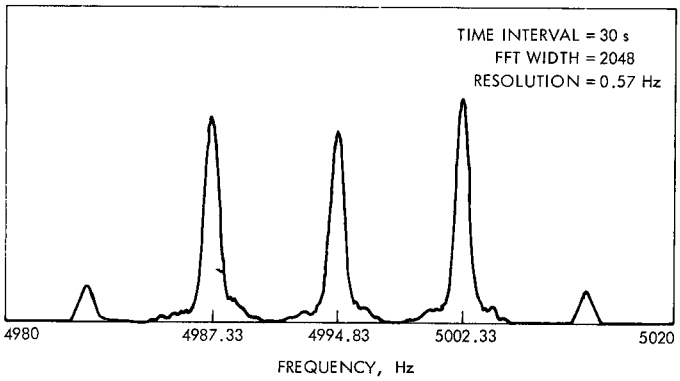

Fig. 1. Power spectrum of timing sinusoid showing flutter sidebands

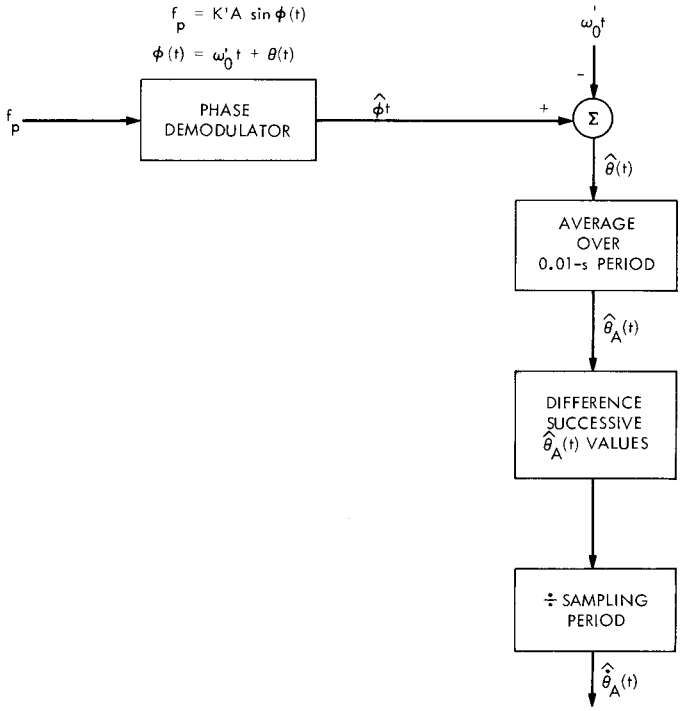

Fig. 2. Block diagram analog of the time domain analysis program

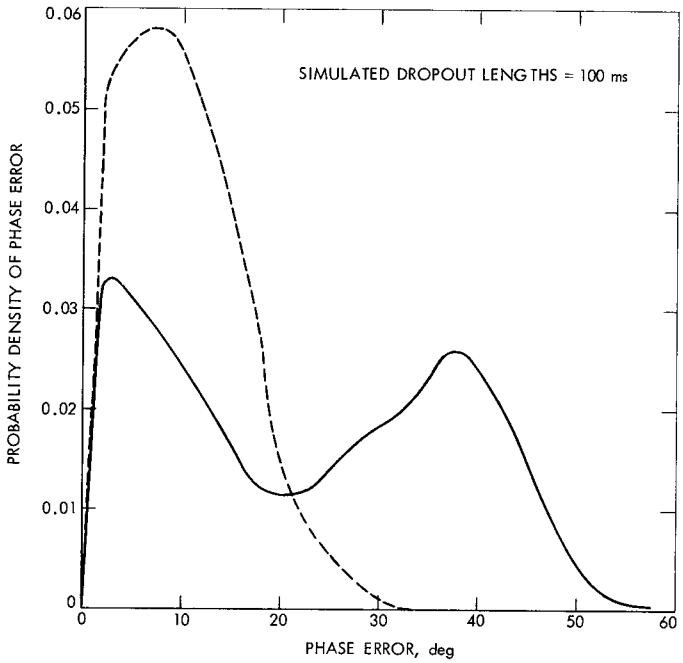

Fig. 3. Probability density of phase error between timing sinusoid and model for two randomly initiated dropouts